🌐 Thieme

Segmental quantification of hepatic lipid content based on volumetric MRI data in patients with suspected iron overload

Quantifizierung des segmentalen Lipidgehalts der Leber auf der Grundlage volumetrischer MRT-Daten bei Patienten mit Verdacht auf Eisenüberladung

Authors
Arthur P. Wunderlich[1, 2]🆔, Holger Cario[3], Stephan Kannengießer[4], Veronika Grunau[1], Michael Götz[2]🆔, Felix Hüttner[5], Johanna Backhus[6], Meinrad Beer[1], Stefan Andreas Schmidt[1]

Affiliations
1 Department for Diagnostic and Interventional Radiology, Ulm University Medical Center, Ulm, Germany
2 Division for Experimental Radiology, Ulm University Medical Center, Ulm, Germany
3 Department of Pediatrics and Adolescent Medicine, Ulm University Medical Center, Ulm, Germany
4 Magnetic Resonance Development, Siemens Healthcare AG, Erlangen, Germany
5 Clinic of Surgery, Ulm University Medical Center, Ulm, Germany
6 Department for Internal Medicine I – Gastroenterology, Ulm University Medical Center, Ulm, Germany

Correspondence
Dr. Arthur P Wunderlich
Clinic for Diagnostic and Interventional Radiology,
University Ulm Medical Centre, Albert-Einstein-Allee 23,
89070 Ulm, Germany
Tel.: +49/7 31/50 06 10 86
Fax: +49/7 31/50 06 11 08
arthur.wunderlich@uni-ulm.de

ABSTRACT

Purpose To investigate the segmental distribution of hepatic fat fraction, determined with MRI (MR proton density fat fraction, short MR-PDFF) in patients suspected of having liver iron overload.

Methods The liver of 44 patients examined with MRI using a 3D multi-echo gradient-echo sequence was segmented semi-automatically and subdivided into nine segments (segment 4 divided in 4a and 4b). Segmental fat content was determined on MR-PDFF maps. Whole-liver steatosis grades were compared to those found in individual segments. Segmental MR-PDFF differences were tested for statistical significance.

Results The most common diseases were thalassemia, various forms of anemia, and hereditary hemochromatosis. No patients suffered from fat metabolism disease. Iron overload was present in 37/44 (84 %) patients. For the whole liver, 22 patients showed a steatosis grade of 0, 21 patients were graded S1, and one patient had a steatosis grade of 2. The grade of steatosis was underestimated in 5 of 21 patients (24 %) in segment 8 and in 8 of 21 patients (38 %) in segment 7. Highly significant segmental MR-PDFF differences were detected with $p < 0.00001$, e. g., comparing segment 2 to 5. Segments 1 to 3 had the highest fat content, segments 7 and 8 had the lowest.

Conclusion Our results suggest that the storage of fat in the liver is inhomogeneous, so that segment-wise differing fat concentrations were found. Fat distribution in patients with suspected hepatic iron overload was similar to living liver donors. However, it showed significant differences compared with the values published for NAFLD patients, which were less pronounced in the group with high average hepatic MR-PDFF values than in the group with normal lipid content. In patients suspected of having iron overload, segment 8, which is mainly targeted for biopsy, and segment 7 may underestimate steatosis grade.

Key Points:
- A volumetric analysis of 3D MRI data of patients with suspected hepatic iron overload yielded a markedly elevated MR proton density fat fraction (MR-PDFF) in hepatic segments 1 to 3.
- This hepatic fat distribution, observed for the whole patient cohort, is similar to healthy living liver donors.

- The subgroup of patients with a high average MR-PDFF ≥ 6.5 % shows this effect with lower segmental deviations.
- In patients without fat metabolic disorders, the steatosis grade may be underestimated when taking biopsies in segment 8 or 7.

ZUSAMMENFASSUNG

Ziel Untersuchung der segmentalen Verteilung des mittels MRT ermittelten hepatischen Fettanteils (MR proton density fat fraction, kurz MR-PDFF) bei Patienten mit Verdacht auf Eisenüberladung der Leber.

Methoden Die Leber von 44 Patienten, die mittels MR mit einer 3D-Multiecho-Gradientenecho-Sequenz untersucht wurden, wurde semiautomatisch segmentiert und in neun Segmente unterteilt (Segment 4 aufgeteilt in 4a und 4b). Der segmentale Fettgehalt wurde anhand von MR-PDFF-Karten bestimmt. Die Steatosegrade der Gesamtleber wurden mit denen der einzelnen Segmente verglichen. Die segmentalen MR-PDFF-Unterschiede wurden auf statistische Signifikanz geprüft.

Ergebnisse Die häufigsten Krankheiten waren Thalassämien, verschiedene Formen von Anämien und hereditäre Hämochromatose. Keiner der Patienten hatte eine Fettstoffwechselstörung. Eine Eisenüberladung lag bei 37/44 (84 %) Patienten vor. Auf die gesamte Leber bezogen hatten 22 Patienten keine Steatose, 21 eine Steatose Grad 1 und ein Patient eine Steatose Grad 2. Der Steatosegrad wurde bei 5 von 21 Patienten (24 %) im Segment 8 und bei 8 von 21 Patienten (38 %) im Segment 7 unterschätzt. Es wurden hochsignifikante segmentale MR-PDFF-Unterschiede festgestellt (p < 0,00001), z. B. beim Vergleich der Segmente 2 und 5. Die Segmente 1 bis 3 hatten den höchsten Fettgehalt, die Segmente 7 und 8 den niedrigsten.

Schlussfolgerungen Unsere Ergebnisse zeigen, dass die Speicherung von Fett in der Leber inhomogen ist, sodass segmental unterschiedliche Fettkonzentrationen gefunden wurden. Die Fettverteilung bei Patienten mit Verdacht auf hepatische Eisenüberladung war ähnlich wie bei Lebend-Leber-Spendern. Sie wies jedoch im Vergleich zu den bereits für NAFLD-Patienten publizierten Werten deutliche Unterschiede auf, die in der Gruppe mit hohen durchschnittlichen hepatischen MR-PDFF-Werten geringer ausgeprägt waren als in der Gruppe mit normalem Fettgehalt. Bei Patienten mit Verdacht auf Eisenüberladung kann in Segment 8, das hauptsächlich Ziel einer erforderlichen Biopsie ist, sowie in Segment 7 der Steatosegrad unterschätzt werden.

Kernaussagen:
- Eine volumetrische Analyse von 3D-MRT-Daten von Patienten mit Verdacht auf hepatische Eisenüberladung ergab einen deutlich erhöhten MR-Protonendichte-Fettanteil (MR-PDFF) in den Lebersegmenten 1 bis 3.
- Diese für die gesamte Patientenkohorte beobachtete hepatische Fettverteilung ähnelt der von gesunden lebenden Leberspendern.
- Die Untergruppe der Patienten mit hoher durchschnittlicher MR-PDFF ≥ 6,5 % zeigte diesen Effekt mit geringeren segmentalen Abweichungen.
- Bei Patienten ohne Fettstoffwechselstörungen kann der Steatosegrad unterschätzt werden, wenn Biopsien in den Segmenten 8 oder 7 entnommen werden.

Introduction

Liver fat content is highly variable in normal subjects and is known to increase in certain metabolic disorders. Using innovative MR sequences, liver fat content can be reliably determined. The so-called MR-based proton density fat fraction (MR-PDFF) has been established as a biomarker [1]. This parameter has been shown to correlate well with liver fat content determined by histology and MR spectroscopy [2]. Liver fat content is certainly of particular interest in metabolic diseases such as non-alcoholic fatty liver (NAFLD). In some of these syndromes, an elevated iron content is also observed, which requires a joint quantification of both substances [3]. Fat content was investigated not only for the whole liver but was also differentiated by segment [4, 5].

On the other hand, iron overload with iron accumulation mainly in the liver, but also in other organs, represents a major problem for patients with chronic anemia. Excess iron is caused by increased iron resorption, frequent blood transfusions, or a combination of both. Since iron overload and its complications can be prevented and treated with iron chelation, noninvasive iron monitoring is crucial for patient management. MRI is widely accepted as the tool for noninvasive liver iron quantification, reflecting the total body iron content. Recently, a three-dimensional multi-gradient echo (3D mGRE) sequence was developed enabling contiguous acquisition of the whole liver in a single breath hold, which offers the possibility of volumetric analysis [6]. Multiple echoes allow for combined quantification of fat and iron [2, 7].

Meanwhile, software solutions are available for semi-automatic liver segmentation including the option to optimize the automatically detected contour manually. One of these tools allows users to divide the liver into its anatomical segments on the basis of manually placed landmarks and to analyze individual segments separately. Using this method, segmental differences in hepatic iron overload, reflected by segmental R_2^* differences, have been found [8].

As fatty liver degeneration is frequently observed in the general population, it also affects patients with chronic anemia [9]. Deviating segmental fat fractions have been reported in fatty liver patients and living liver donors in single slice ROI-based analysis

[4, 5]. The question remains whether there are also differences in segmental fat fraction in hematologic patients. So far, it is unknown whether similar segmental fat fraction differences exist in patients with hereditary hemochromatosis or anemia-associated iron overload. Since the 3D mGRE sequence mentioned above makes it possible to assess not only iron concentration but also fat fraction, this study aimed to evaluate the segmental distribution of hepatic MRI proton density fat fraction (MR-PDFF) in patients with suspected iron overload based on volumetric MRI data.

Methods

After approval by the university's ethics committee and according to the Declaration of Helsinki (last revision 2013, Fortaleza, Brazil), patients referred to our institution between May 2017 and April 2018 for noninvasive liver iron quantification were included after written informed consent of the patients and/or their parents. Participants were examined on a 1.5 T MRI scanner (MAGNETOM Avanto, Siemens Healthcare, Erlangen, Germany) with a volumetric multi-gradient echo research sequence (6 echoes, TEs 1.2–9 ms) as previously published [8, 10]. The entire liver was acquired in a single breath hold with a field of view (FoV) of 400x300x224 mm^3 at a matrix of 160x84x56 voxels and a voxel size of 2.5x2.5x4 mm^3. Immediately after data acquisition, voxel-by-voxel PDFF and R_2^* values were obtained using a nonlinear multi-step fit process and stored as a parameter map [1].

Image quality was scored using a four-point Likert scale with 1 = excellent image quality, 2 = marginal artifacts not compromising liver diagnosis, 3 = image quality impaired by breathing and/or fat-water mismatch (so called swaps) and 4 = severe image artifacts. Patients in whom the liver was not completely covered, e. g., due to a different breathing position compared to the survey slices or because the liver was not completely depicted in these, and patients with poor image quality (Likert score 3 or 4) of the volumetric sequence were excluded from analysis.

Liver segmentation was performed using the Liverhealth software tool, a part of the Intellispace Portal (ISP, Philips, Hamburg, Germany) which was described previously [8, 10]. The liver contour on axial slices as well as coronal and sagittal reconstructions was checked after an initial automatic segmentation and corrected manually if necessary. Subsequently, the liver was subdivided into segments using manually marked anatomical landmarks. We used the subdivision according to Couinaud/Bismuth with a total of 9 segments with differentiation of segment 4 into 4a and 4b. The landmarks required by the software for the segment division were: right portal bifurcation, inferior vena cava, right and middle hepatic vein, umbilical fissure, left portal bifurcation, left hepatic apex, superficial venous ligament, attachment of venous ligament to portal vein, and attachment of venous ligament to vena cava. Mean values of MR-PDFF and R_2^* were stored for the whole liver and for individual segments. A scatterplot of whole-liver MR-PDFF vs. R_2^* values was created and the correlation between these values was studied.

Liver steatosis was graded based on the whole-liver MR-PDFF values according to the recently proposed thresholds [11]. An evaluation was performed to determine whether assessment of single segments would over- or underestimate steatosis grade. Furthermore, the number of patients in whom segments 7 and 8 show lower MR-PDFF values than the average whole-liver MR-PDFF was assessed. Iron overload was addressed using the average whole-liver R_2^* value and a recently published calibration for the sequence was used [7].

PDFF values of the segments were normalized by dividing each segmental value by the PDFF value of the whole liver according to

$$rFF_{Seg} = \frac{PDFF_{Seg}}{PDFF_{Liv}}$$

where $PDFF_{Seg}$ denotes PDFF measured in a single segment, $PDFF_{Liv}$ means PDFF averaged over the whole liver, and rFF_{Seg} the relative PDFF value of a single segment.

Segmental PDFF and the normalized, or relative, PDFF values (rFF) were averaged segment by segment for all patients and tested for differences between the segments. This was performed for all patients together and for patients divided into two groups according to their average hepatic MR-PDFF value. The cutoff value was set to 6.5 %, a threshold value that is suitable to differentiate between normal and steatotic liver [11]. Furthermore, relative segmental values were studied for differences between patients solely with increased iron resorption like those with hereditary hemochromatosis, patients with chronic hemolytic anemia not receiving blood transfusions, and anemia patients requiring frequent blood transfusion.

All statistical analyses were done using SPSS software (version 27.0, IBM, Armonk/NY, USA). All variables were initially tested for normal distribution using the Shapiro-Wilk test. The relative values rFF of the individual segments were tested for statistically significant differences using analysis of variance with repeated measures (ANOVA) and Bonferroni correction. The test for variance homogeneity required for ANOVA was performed using Mauchly's test followed by Greenhouse-Geisser's epsilon factor correction.

Significance levels for statistical analyses were set to $p < 0.05$ for significant and $p < 0.001$ for highly significant differences.

Results

58 participants were examined in the chosen time interval. No patient had a known fat metabolism disease. The liver was imaged completely in all cases. 30/58 (52 %) of the studies were scored 1 for excellent image quality, and 14/58 (24 %) received a Likert score of 2. A total of 14/58 participants (24 %) had to be excluded, 10 received a score of 3 and 4 were scored 4. Therefore, 44 patients (24 m, 20f, age 23.7 ± 13 years (mean ± SD), age range 4.1 to 60.6 years) were suitable for evaluation. ▶ **Fig. 1** shows a color-coded MR-PDFF map overlaid on an anatomical image.

The two disease patterns most frequently observed in our patient cohort were transfusion-dependent thalassemia (n = 24) and Diamond-Blackfan anemia (n = 5). Other diseases and their frequency are shown in ▶ **Table 1**. ▶ **Fig. 2** shows a dot plot of MR-PDFF vs. R_2^* with moderate correlation of both parameters.
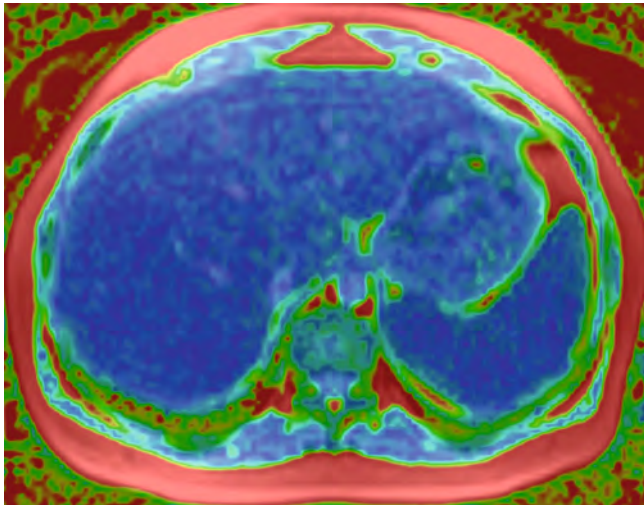
▶ **Fig. 1** Color-coded MR-PDFF map overlaid on an anatomical image. MR-PDFF was coded in colors as follows: blue: lowest, green: intermediate, yellow/red: highest.

▶ **Table 1** Disease patterns, sorted with respect to blood transfusions, and number of participants split by gender.

Disease	Male	Female	Sum
Patients receiving blood transfusions			
Thalassemia	11	13	24
Diamond-Blackfan anemia	3	2	5
Leukemia after bone marrow transplant	1	1	2
MDS after bone marrow transplant	1	1	2
Sickle cell disease	0	1	1
Congenital hemolytic anemia	0	1	1
Severe aplastic anemia	0	1	1
Osteopetrosis	1	0	1
No blood transfusions			
Primary hemochromatosis	4	0	4
Pyruvate kinase deficiency	1	0	1
Congenital dyserythropoietic anemia	1	0	1
Hemolytic anemia due to Hb Youngstown	1	0	1
Sum	**24**	**20**	**44**

Whole-liver MR-PDFF values ranged from 3.6 % to 20 %. For individual segments, we found a range of 2.9 % to 21.1 %. Average segmental MR-PDFF values for different patient groups are given in ▶ **Table 2**. Relative PDFF values were observed between 0.51 and 1.87.

All patients showed a lower segmental MR-PDFF compared to the average whole liver MR-PDFF in either segment 7 or 8. Reduced values were observed in 38/44 patients (86.4 %) for segment 7 and in 37/44 patients (84.1 %) for segment 8.

In 22 patients a steatosis grade of 0 (S0) was found (MR-PDFF < 6.5 %), 21 were graded S1 (MR-PDFF 6.5–16.5 %), and one patient was graded S2 (MR-PDFF 16.5–22 %). No patient was graded S3 (MR-PDFF > 22 %). In 11 of 22 patients (50 %) graded S0, segment 2 showed an S1 grade, in 2 of 21 patients (9.5 %) with whole-liver steatosis grade S1, segment 2 was graded S2. On the other hand, 5 of 21 patients (24 %) with whole-liver grade S1 were graded S0 in segment 8. These five patients and three additional patients, i. e., a total 8 of 21 (38 %) were graded S0 in segment 7. Only two of 21 patients (9.5 %) with whole-liver grade 1 were graded S0 in segment 5, and only one patient in the steatosis group S1 was graded S0 in segment 4a and another in segment 4b.

Liver iron overload was detected in 37/44 (84 %) patients.

▶ **Fig. 3** shows an overview of average rFF values of individual segments. Highly significant differences were found between segments 1 to 3 versus segments 4a-8. Also, highly significant differences occurred between segments 4a versus segments 7 and 8. Significant differences were also observed between segment 4b versus segments 5, 7, and 8, and between segment 5 versus 8 and segment 6 versus 7. The p-values of the segment-wise differences are shown in ▶ **Table 3** for rFF and actual MR-PDFF.

Segmental rFF values of the two patient groups separated according to MR-PDFF are shown in ▶ **Fig. 4, 5**. Note the reduced rFF values of segments 1–3 in the high average MR-PDFF group com-

pared to the low MR-PDFF group, whereas other segments in this comparison tend to show increased rFF values. In other words, the inter-segmental differences are reduced in the patients with steatosis (steatosis grade > 0) compared to patients without steatosis. This effect is borderline not significant in S2 (p = 0.052) but significant in S4b (p = 0.044) and S8 (p = 0.040).

▶ **Fig. 6** shows rFF values of patients with solely increased iron resorption without blood transfusions (n = 7, all male) as compared to patients who needed frequent blood transfusions. Significant differences between these groups were found in segments 4b (p = 0.015) and 7 (p = 0.013).

Discussion

Liver fat content has been the subject of several studies, but, so far, mainly in patients with lipid metabolic diseases such as nonalcoholic fatty liver disease (NAFLD). Here, we investigated hepatic fat content in patients with hereditary hemochromatosis or anemia-associated iron overload. The resulting liver iron overload is measured by the transverse relaxation rate R_2^*. R_2^* distribution deviated from PDFF distribution: R_2^* is lowest in segment 1 and highest in segment 7 [8, 10]. Since relative segmental MR-PDFF values do not correspond to relative segmental R_2^*, we conclude that our method determines these values independently from each other. Therefore, the observation that MR-PDFF correlates moderately to R_2^* is assumed to have physiologic or pathologic reasons.

A study in healthy living liver donors showed fat fractions comparable to those in our patients, i. e., highest fat content in seg-
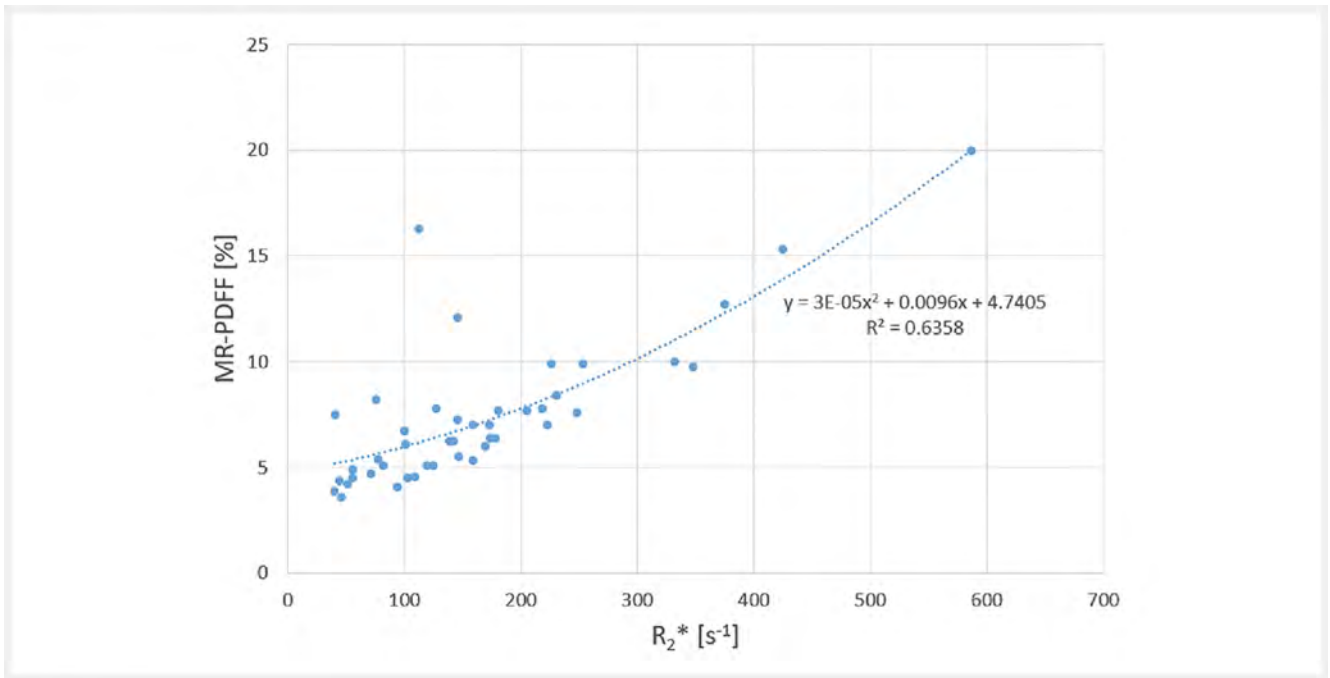
► **Fig. 2** Scatterplot of whole-liver MR-PDFF vs. R_2^*. The quadratic equation describes the relationship best. Correlation is only moderate.

ments 1–3, but with overall lower MR-PDFF values [4]. These observations suggest that fat distribution obviously depends on the individual condition, i. e., healthy persons or patients with suspected liver iron overload vs. patients with lipid metabolic diseases. In practice, this might be important when taking biopsies from patients with suspected iron overload in order to evaluate steatosis grade since the right liver lobe (segment 8) is mainly targeted. It might be helpful to target segment 5 instead, but this is associated with a higher risk of complications.

Increased fat storage in the right liver lobe compared to the left liver lobe, i. e., exactly the opposite as observed in the studied patient cohort, has already been reported for NAFLD patients in several papers, although mostly only whole liver lobes and not individual segments were examined [3, 12]. Studies investigating fat distribution using the Coinaud/Bismuth segmental subdivision in NAFLD patients found a lower fat content in segments 1–3 compared to the other segments [2, 5, 13]. This is remarkable since both conditions, iron overload as well as NAFLD, are associated with increased hepatic fat content. The fat content within the extended right lobe of the liver (segments 4 to 8) reported by these studies, however, are comparable to results observed in our patient population, i. e., highest in segment 4 and with a decreasing tendency toward segment 8 with basically similar MR-PDFF values. The comparison between patients with normal MR-PDFF < 6.5 % and steatotic patients (MR-PDFF ≥ 6.5 %) in our collective shows that with increasing hepatic fat content, fat tends to accumulate more in segments 5–8 compared to segments 1–3.

Patients in our cohort who did not receive blood transfusions suffered from excess iron due to increased iron resorption. The pattern of cellular iron distribution in the liver differs from that in patients with secondary transfusional iron overload for several reasons. This includes, e. g., the primary portal circulation after iron resorption and the high hepatocellular TFR2 expression [14]. Therefore, in hereditary hemochromatosis and non-transfusion-dependent anemias, iron primarily accumulates in hepatocytes, whereas in transfusional iron overload cells of the reticulo-histiocytic system including hepatic stellate cells are affected. In the group requiring blood transfusions, aged blood cells are metabolized by the hepatic reticulo-endothelial system and not by hepatocytes. Examining segmental MR-PDFF, probable effects of these differences are seen. However, it remains unclear why significant differences occur only in segments 4b and 7. Since our group without blood transfusions was small (n = 7), we regard this result as preliminary. The larger group receiving blood transfusions could be spit up further into patients with additionally increased iron resorption (thalassemia) and iron overload predominantly caused by blood transfusion (sickle cell disease, Diamond-Blackfan anemia and other forms of anemia). Interestingly, despite segmental R_2^* values differing between these groups [8], there were no significant segmental MR-PDFF differences between the subgroups (data not shown).

Limitations

This study was conducted as a feasibility study on a rather small number of patients. In particular, the patient group with solely increased iron resorption was very small. Furthermore, due to image quality, especially fat-water swaps, 24 % of the actually

▶ **Table 2** Segmental actual (not relative) values MR-PDFF [%] for different patient groups (mean ± Std. Dev.).

	Segment 1	Segment 2	Segment 3	Segment 4a	Segment 4b	Segment 5	Segment 6	Segment 7	Segment 8
All patients	8.96±3.4	9.30±3.7	9.22±3.5	7.26±3.4	7.82±3.8	7.05±3.5	6.95±3.8	6.22±3.4	6.61±4.2
MR-PDFF <6.5%	6.74±1.6	6.75±1.1	6.82±1.4	5.16±1.3	5.13±1.4	4.65±1.0	4.71±1.3	4.27±1.1	4.20±1.2
MR-PDFF ≥6.5%	11.2±3.4	11.9±3.7	11.6±3.2	9.35±3.6	10.5±3.5	9.46±3.5	9.20±4.1	8.16±3.8	9.01±4.8
Patients solely with increased iron resorption	9.69±4.2	10.8±5.4	9.79±4.4	8.13±3.6	7.37±3.8	7.17±2.7	8.17±2.6	8.04±3.7	8.59±6.2
Patients who received blood transfusions	8.82±3.3	9.03±3.4	9.12±3.3	7.09±3.4	7.91±3.9	7.03±3.7	6.72±3.9	5.87±3.2	6.24±3.8
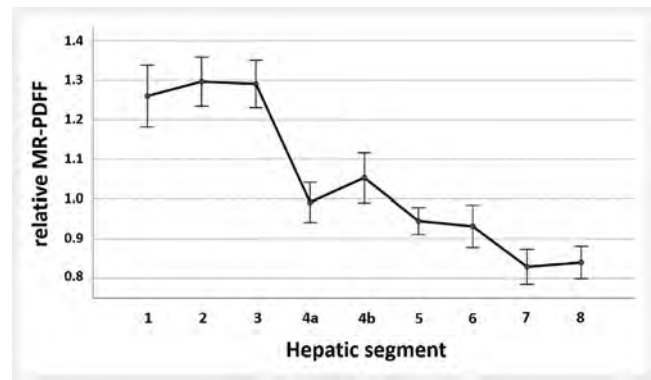
▶ **Fig. 3** Relative segmental MR-PDFF values shown with their 95 % confidence interval for all patients. Note the marked difference between segments 1–3 and the others.

scanned patients had to be excluded from analysis. The volumetric sequence used, particularly the inline fitting process, was a research version. In the meantime, processing was optimized to minimize errors like fat-water swaps [15]. First experiences with the most recent product version let us expect fewer cases not suitable for analysis in the future.

Nonuniform distribution of MR-PDFF was studied segment by segment in a first step. We are aware of the fact that there is nonuniformity also within segments. A more elaborate analysis would be necessary to further study the uniformity of MR-PDFF distribution on a shorter length scale.

There was no accompanying investigation into potential technical confounders contributing to the observed segmental differences. Noise floor effects in combination with a spatially varying SNR of local coil arrays and parallel imaging could lead to a segment-dependent bias in the PDFF values. However, review of the individual echo images showed that at most the two largest echo times suffer from an insufficient signal. We performed signal simulations and parameter fitting with these boundary conditions (data not shown) which indicate primarily larger uncertainties, i. e., reduced precision, of single-voxel MR-PDFF values, which we expect to average out when considering whole hepatic segments. Some bias was also predicted, with a tendency to overestimate low MR-PDFF and underestimate high MR-PDFF values. Therefore, there may be even larger segmental differences than reported here. The bias effects are stronger for a lower SNR, but primarily for very low MR-PDFF and very high R_2^*, a combination not observed in our patients. In particular, it can be ruled out that the segmental differences for patients with elevated MR-PDFF ≥ 6.5 % (▶ **Fig. 4**) are caused by a spatially varying SNR.

We only studied patients suspected of having iron overload. To address effects arising from elevated liver fat, it would be of interest to additionally investigate individuals without liver impairment, receiving MR abdominal scans for other reasons. In this study, however, we focused on patients suspected of having hepatic iron overload. The effects of increased liver fat were studied by dividing patients into two groups according to their hepatic fat content, related to liver steatosis. This may have caused a selection bias. Therefore, results should be interpreted with caution.

► **Table 3** p-values for significance of differences between individual segments (row vs. column) for actual and relative (given in parenthesis) MR-PDFF values for the whole patient cohort. Only significant and highly significant values are given. For other combinations, i. e., segment 1 vs. S2 or S3, and S7 vs. S8, the differences were not significant.

	Segment 4a	Segment 4b	Segment 5	Segment 6	Segment 7	Segment 8
Segment 1	0.00004 (0.00001)	0.006 (0.0012)	0.000004 (0.000002)	0.000007 (0.000003)	<0.000001 (<0.000001)	0.00002 (<0.000001)
Segment 2	0.000003 (<0.000001)	0.0005 (0.00003)	<0.000001 (<0.000001)	<0.000001 (<0.000001)	<0.000001 (<0.000001)	<0.000001 (<0.000001)
Segment 3	<0.000001 (<0.000001)	0.000003 (<0.000001)	<0.000001 (<0.000001)	<0.000001 (<0.000001)	<0.000001 (<0.000001)	<0.000001 (<0.000001)
Segment 4a	–	–	–	–	0.0007 (0.00019)	– (0.00011)
Segment 4b	–	–	– (0.0051)	–	0.0011 (0.00082)	– (0.00043)
Segment 5	–	–	–	–	–	– (0.005)
Segment 6	–	–	–	–	– (0.015)	–
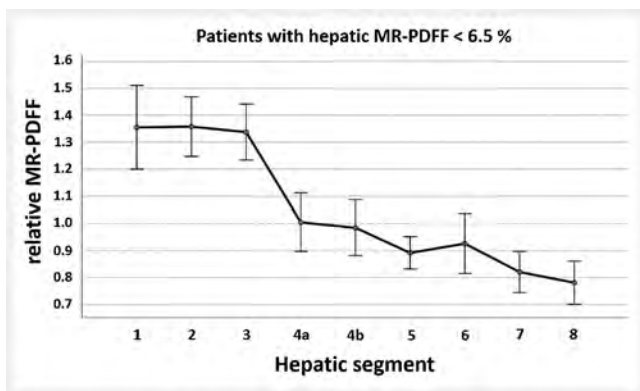
► **Fig. 4** Relative segmental MR-PDFF (rFF) values shown with their 95 % confidence interval for patients with normal MR-PDFF < 6.5 %. Note the elevated rFF in segments 1–3 compared to all patients (► **Fig. 3**).
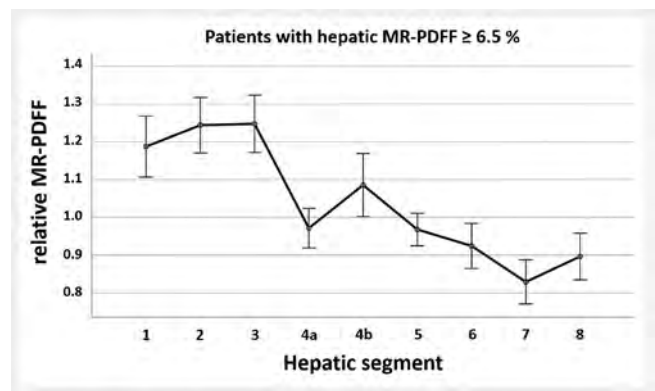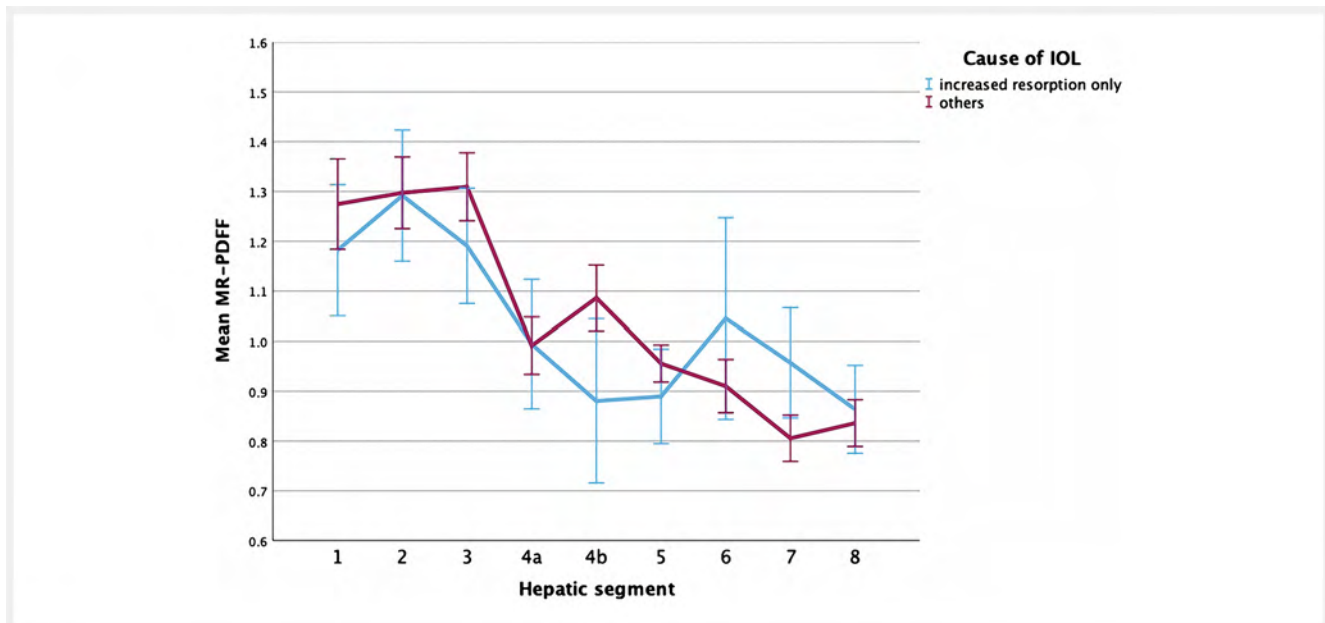

► **Fig. 5** Relative segmental MR-PDFF values shown with their 95 % confidence interval for patients with elevated MR-PDFF ≥ 6.5 %. Note the reduced segmental deviations, except for segment 4b, compared to patients with normal MR-PDFF (► **Fig. 4**).

Conclusion

Our data indicate that the storage of fat in the liver is inhomogeneous, so that differing segmental fat concentrations are found. This should be verified in a larger number of patients. This important observation may also have a practical impact, for example, for targeting liver biopsy to evaluate steatosis grade and other impairments like inflammation. This should be investigated in further clinical studies.

CLINICAL RELEVANCE

- Contiguous 3D MRI data of patients with suspected hepatic iron overload showed a markedly elevated MR proton density fat fraction (MR-PDFF) in hepatic segments 1 to 3 in a volumetric analysis.
- In patients suspected of having iron overload, intrahepatic fat distribution is similar to that of healthy persons.
- Steatosis grade may be underestimated in patients without fat metabolic disorders when taking biopsies in hepatic segment 7 or 8.

▶ **Fig. 6** Relative segmental MR-PDFF values shown with their 95 % confidence interval for patients solely with increased iron absorption, who did not receive any blood transfusion (blue), and patients where blood transfusions were necessary due to their disease (red). Significant differences between these groups were observed in segments 4b ($p = 0.015$) and 7 ($p = 0.013$).

Conflict of Interest

Acknowledgement

References

[1] Zhong X, Nickel MD, Kannengiesser SA et al. Liver fat quantification using a multi-step adaptive fitting approach with multi-echo GRE imaging. Magn Reson Med 2014; 72: 1353–1365

[2] Kang BK, Kim M, Song SY et al. Feasibility of modified Dixon MRI techniques for hepatic fat quantification in hepatic disorders: validation with MRS and histology. Br J Radiol 2018; 91: 20170378

[3] Hui SCN, So HK, Chan DFY et al. Validation of water-fat MRI and proton MRS in assessment of hepatic fat and the heterogeneous distribution of hepatic fat and iron in subjects with non-alcoholic fatty liver disease. Eur J Radiol 2018; 107: 7–13

[4] Choi Y, Lee JM, Yi NJ et al. Heterogeneous living donor hepatic fat distribution on MRI chemical shift imaging. Ann Surg Treat Res 2015; 89: 37–42

[5] Bonekamp S, Tang A, Mashhood A et al. Spatial distribution of MRI-Determined hepatic proton density fat fraction in adults with nonalcoholic fatty liver disease. J Magn Reson Imaging 2014; 39: 1525–1532

[6] Breuer FA, Blaimer M, Mueller MF et al. Controlled aliasing in volumetric parallel imaging (2D CAIPIRINHA). Magn Reson Med 2006; 55: 549–556

[7] Wunderlich AP, Schmidt SA, Mauro V et al. Liver Iron Content Determination Using a Volumetric Breath-Hold Gradient-Echo Sequence With In-Line R(2) * Calculation. J Magn Reson Imaging 2020; 52: 1550–1556

[8] Wunderlich AP, Cario H, Kannengießer S et al. Volumetric Evaluation of 3D Multi-Gradient-Echo MRI Data to Assess Whole Liver Iron Distribution by Segmental R2* Analysis: First Experience. Fortschr Röntgenstr 2023; 195: 224–233

[9] Szczepaniak LS, Nurenberg P, Leonard D et al. Magnetic resonance spectroscopy to measure hepatic triglyceride content: prevalence of hepatic steatosis in the general population. Am J Physiol Endocrinol Metab 2005; 288: E462–E468

[10] Wunderlich AP, Kannengießer S, Grunau V et al. 3D multi-echo GRE MRI of the whole liver: First experiences of a volumetric segmental R2* analysis. ISMRM Annual Meeting; 2022; London

[11] Dioguardi BurgioM, Imbault M, Ronot M et al. Ultrasonic Adaptive Sound Speed Estimation for the Diagnosis and Quantification of Hepatic Steatosis: A Pilot Study. Ultraschall in Med 2019; 40: 722–733

[12] Hua B, Hakkarainen A, Zhou Y et al. Fat accumulates preferentially in the right rather than the left liver lobe in non-diabetic subjects. Dig Liver Dis 2018; 50: 168–174

[13] Lee H, Jun DW, Kang BK et al. Estimating of hepatic fat amount using MRI proton density fat fraction in a real practice setting. Medicine 2017; 96: e7778

[14] Muñoz M, Villar I, García-Erce JA. An update on iron physiology. World J Gastroenterol 2009; 15: 4617–4626

[15] Henninger B, Plaikner M, Zoller H et al. Performance of different Dixon-based methods for MR liver iron assessment in comparison to a biopsy-validated R2* relaxometry method. Eur Radiol 2021; 31: 2252–2262